J Mol Model (2011) 17:2773–2780
DOI 10.1007/s00894-010-0946-7

ORIGINAL PAPER

Adsorption mechanism of single guanine and thymine on single-walled carbon nanotubes

Muthusivarajan Rajarajeswari · Kombiah Iyakutti · Yoshiyuki Kawazoe

Received: 2 November 2010 / Accepted: 27 December 2010 / Published online: 29 January 2011

Abstract Bio-nano hybrids introduce magnificent applications of nanomaterials to various fields. The choice of carbon nanotube as well as sequence selection of the nucleic acid bases play a crucial role in shaping DNA–carbon nanotube hybrids. To come up with a clear vision for the choice of carbon nanotube and nucleic acid bases to create bio-nano hybrids, we studied the adsorption mechanism of the nucleic acid bases guanine and thymine on four different types of nanotubes based on density functional theory. Nucleic acid bases exhibit differential binding strengths according to their structural geometry, inter-molecular distances, the carbon nanotube diameter, and charge transfer. The π–π interaction mechanism between the adsorbent and adsorbate is discussed in terms of charge density profile and electronic band structure analysis.

Keywords Carbon nanotube · Nucleic acid base · π–π stacking interaction · Density functional theory

Introduction

The study of the noncovalent interactions of biological molecules with single-walled carbon nanotubes (SWCNT) has emerged as a separate field in nanotechnology. Functionalization of CNT with biomolecules leads to many potential applications in medicinal biology as well as in solid state nano electronics. Carbon nanotubes are being explored as one of the most promising transfection vectors for drug and gene delivery, due to their large surface area, stability, flexibility and biocompatibility. Hybrids of SWCNT-ribonucleic acid (RNA) polymer formed through nonspecific binding are translocated into MCF7 breast cancer cells with radioscope labeling [1]. SWNTs have the ability to penetrate mammalian cells as intracellular protein transporters with noncovalently bound protein cargo [2]. An electronic biosensor for detecting antibodies associated with human autoimmune diseases has been developed through the nonspecific binding of proteins on carbon nanotubes [3]. Carbon nanotubes decorated with peptide is used in a field effect transistor (FET)-based chemical sensor to detect specific targets using peptide recognition elements [4].

Deoxyribonucleic acid (DNA) overstated its role not only in biology, but also in nanotechnology. Integration of carbon nanotubes with the genetic material DNA opens up several possible applications of CNT in the field of bio-nanotechnology. Over a decade of research has now contributed to our understanding of the interactions in DNA–CNT hybrids. Nonspecific interaction of CNTs with DNA helps the dispersion and separation of CNTs in aqueous and non-aqueous solution, while leaving the unique physical and electronic properties of CNTs unchanged. The helical wrapping of poly(T) on a carbon nanotube (10, 0) converts CNT into a water soluble object and helps to sort the carbon nanotubes with respect to their electronic properties [5]. Self-assembly of the sequence $d(GT)_n$ around individual nanotubes enables nanotube separation using ion exchange liquid chromatography [6, 7]. In the study of a

M. Rajarajeswari · K. Iyakutti (✉)
School of Physics, Madurai Kamaraj University,
Madurai, Tamil Nadu 625 021, India
e-mail: iyakutti@yahoo.co.in

Y. Kawazoe
Institute for Materials Research, Tohoku University,
Sendai 980-8577, Japan

molecular dynamics simulation of a self-assembly of random sequence ssDNA on CNT, achiral loops and disordered kinked structures are observed due to the flexibility of ssDNA [8]. Also, the helical wrapping of poly (GT) on CNT [6, 7] is claimed to be structurally unstable, and the oligonucleotide does not prefer to be adsorbed onto CNTs as a dimer. "Ultrasoft" DNA sequencing have been performed by detecting the variation in the current through a CNT when different DNA base pairs are in contact with the CNT [9]; the individual nucleosides adsorbed on the CNT are also identified with the applied external gate voltage [10]. These results shows that the adsorption mechanism of nucleic acid bases on CNT varies with respect to each nucleic acid base. Depending on the length and the sequence of nucleic acid bases in the DNA, a large molecular library is available from which to produce a number of DNA–CNT hybrids, leading to a wider range of magnificent applications. In its simplest form, individual nucleic acid bases can interact with CNTs singly or in multiples (poly). Interactions of isolated nucleic acid bases with CNTs have been studied using density functional theory (DFT) with different functionals [11, 12], and with Raman spectroscopic technique [13]. Das et al. [14] investigated the binding of nucleobases with CNT by means of Hartree-Fock (HF) theory and isothermal calorimetry experiments. Atomistic molecular dynamics (MD) simulations were performed to study the binding of nucleotide monophosphates with (6, 0) SWCNTs in aqueous solution [15]. From previous reports, it is clear that generally binding of DNA to CNT depends generally on the nucleotide sequence and the nanotube diameter [16].

In earlier reports, binding energies of all five nucleic acid bases with a carbon nanotube is calculated using different density functional codes [11–17]. Interaction strength varies in the order G>A>T>C>U [11, 13, 14]. Self-stacking interactions of nucleobases compete with the cross-stacking interaction strength of nucleobases with CNT [18]. Thus, the interaction strength of nucleobases with CNT should be able to overcome the self-stacking interactions. Using ion exchange chromatography technique, Zheng et al. [5–7] proved the ability of poly (T) and poly (GT) to disperse CNTs in aqueous solution. Of the four nucleobases, from the relative binding energies of self-stacking nucleobases and cross-stacking on CNT, Wang [18] proved that thymine can disperse CNT in aqueous solution better than adenine and cytosine. Consequently, the nucleic acid bases thymine and guanine have gained importance in the dispersion of CNTs. Like the differential adsorption strength of nucleic acid bases, different chiralities of CNT also play a significant role in the binding strength of CNT–nucleic acid base hybrids. Earlier reports concentrated on finding the variation in binding energies of different nucleic acid bases with a CNT. Some reports presented electronic band structure analysis and iso surface charge density plots [11, 17], and examined the interaction between them. However, we choose to investigate the role of the curvature and chirality of the CNT in the formation of DNA–CNT hybrid. In our study, to expand our knowledge of the interaction between the nucleic acid bases thymine and guanine and CNTs of different chiralities, with the help of standard density functional code, we present the role of geometry, adsorption mechanism, charge transfer, electronic band structure analysis and charge density analysis.

Computational details

Calculations were carried out using DFT with a plane wave basis set as implemented in the Vienna ab-initio simulation package (VASP) [19, 20]. The projected augmented-wave method (PAW) is used to describe the interaction between ions and electrons [21]. The PAW method has two advantages over ultrasoft pseudo potentials (USPP). It provides all-electron wave functions for valence electrons and shows a better convergence behavior than USPP [21]. DFT is used to describe the ground state properties of many-body systems. Exchange correlation energy can be evaluated with the help of local density approximation (LDA) [22] or with generalized gradient approximation (GGA) [23]. Non-covalent interaction between the two systems is the result of van der Waals, hydrogen bonding, ion-pairing, cation–π and π–π interactions. It is well known that neither LDA nor GGA can describe weakly bound systems perfectly. A considerable effect of exchange correlation energy functionals in the binding energy was noted with DFT techniques. Generally, LDA overestimates the interaction energy of weakly bound systems and GGA underestimates it. Here, our aim was to study non-covalent interactions between DNA–CNT hybrids, thus we had to be very precise in choosing an exchange correlation functional with which to determine accurate interaction energies and structural properties. DFT-LDA calculations underestimate dispersion energy at large distances but can reproduce the empirical potential for graphitic structures successfully [24]. Studies on self-stacking of benzene and cross stacking of benzene on graphene sheet within GGA have shown almost no binding energy [25]. However, the interlayer distance for adenine adsorption on graphene sheet reported using the DFT-LDA technique is very close to the experimental result [26]. Most recently, Lim and Park [27] have investigated the noncovalent adsorption of aromatic molecules on CNT with the help of LDA, GGA and hybrid functionals. It was found that DFT-LDA and M06 hybrid functionals produce almost equal binding energy, and that GGA fails to predict the noncovalent interaction. With this

previous literature support, we decided to follow the LDA approach to investigate the exchange correlation energy of our weakly bound systems.

For k-points sampling of the brillouin zone, a 1×1×4 Monkhorst-Pack grid [28] is used with a spacing of 0.025 $Å^{-1}$. For the electronic band structure calculations, 41 irreducible k-points are considered along the *z*-axis direction. Cutoff energy for the plane wave basis set of the valence electron was fixed as 500 eV throughout the calculations. Residual minimization / direct inversion in the iterative subspace method (RMM–DIIS) is used for wave function optimization. Geometry optimization was carried out until the magnitude of the forces acting on all atoms was smaller than 0.0005 eV/Å. The CNTs zigzag (5, 0), (10, 0), armchair (5, 5) and chiral (5, 2) were used in this study. The number of unit cells of CNT is limited by the height of the nucleic acid bases. In all four cases, approximately 20 Å distance is kept between adjacent tubes to avoid interactions between them. Thymine and guanine are nucleic acid bases found in the genetic material DNA. Thymine is a pyrimidine nucleobase, having one hexagon ring with two nitrogen atoms. Guanine is a derivative of purine consisting of a fused pyrimidine-imidazole system with conjugated double bonds. Initially, the hexagon of the nucleic acid base is kept head-to-head with the hexagon of the carbon nanotube. The plane of the nucleic acid base is parallel with the nanotube *z*-axis direction. Atoms are allowed to relax freely in all directions, to determine the possible adsorption positions of nucleic acid bases on the CNT surface.

Results and discussion

Geometry and energetics of adsorption of guanine and thymine on SWCNTs

Prediction of accurate interaction energy of the adsorbate with the adsorbent involves description of intermolecular parameters such as the orientation of the adsorbate, and inter-molecular distances between the adsorbent and adsorbate. These parameters play a significant role, especially in the case of non-covalent interactions. During geometry optimization, the initial orientation of nucleic acid bases on CNTs was altered to attain the minimum energy configuration, but the nucleic acid bases are still parallel to the nanotube surface. The distance between the CNT and each nucleic acid base is measured from the center of the hexagonal ring of the adsorbate to the nanotube surface. Binding energies, equilibrium distances and charge transfer from the nucleic acid bases to the CNT are presented in Table 1. There is no chemical bond formation between the systems and the binding energies confirm that the process is physisorption. The oxygen and nitrogen atoms of nucleic acid bases have lone pairs of electrons and, due to the sp^2 hybridization of carbon atoms in the CNT, each carbon atom possesses one delocalized p electron. These π electrons lead to physisorption of the nucleic acid bases on the CNT.

Intermolecular distances between the CNT and the nucleic acid bases guanine and thymine vary between 2.46 and 3.26 Å. These values are comparable to those reported in previous studies [13, 17]. Among the four nanotubes, thymine is adsorbed close to CNT (10, 0) at a distance of 2.46 Å, which is less than the characteristic π–π stacking distance. Intermolecular separation of adenine on graphite surface is reported as 3.1 Å within LDA, and AFM studies give the same value [26]. As reported by Stepanian et al. [13], the difference between intermolecular distances estimated using second-order Moller-Plesset perturbation theory (MP2) and DFT is about 0.02 Å. Thus, the calculated intermolecular separation of a non-covalently bound system using DFT-LDA is comparable with the results obtained from experiments and MP2 methods. Adsorption of nucleic acid bases on CNT resembles AB stacking between graphene layers. The orientation of nucleic acid bases on the surface of the CNT differs with

Table 1 Binding energies, charge transfer, equilibrium distances for the adsorption of guanine and thymine on carbon nanotubes (CNTs), and diameter of CNTs

System	Binding energy (E_b, eV)	Charge transfer from nucleic acid base (q, e)	Distance (d, Å)	Diameter (d_t, Å)
CNT (5, 0)+Guanine	0.41	0.094	3.07	3.96
CNT (5, 2)+Guanine	0.36	0.009	3.05	4.95
CNT (5, 5)+Guanine	0.38	0.001	2.98	6.87
CNT (10, 0)+Guanine	0.39	0.008	3.06	7.94
CNT (5, 0)+Thymine	0.20	0.026	3.26	3.96
CNT (5, 2)+Thymine	0.26	0.005	2.95	4.95
CNT (5, 5)+Thymine	0.30	0.009	2.97	6.87
CNT (10, 0)+Thymine	0.20	0.014	2.46	7.94

CNT chirality so as to attain the minimal energy configuration.

The binding energy of guanine with a narrow nanotube (5, 0) is 0.41 eV, and the tube becomes compressed in the direction of the adsorbate. The radius of the tube is reduced to 1.87 Å in the strained direction (Fig. 1a,e). In studies of interaction between nanotubes and biomolecules, to reduce the computational expense, fragmented CNTs have been used [13, 18]. Fragmenting material such as high-curvature CNT may not give reliable results. Wang [18] examined the adsorption of DNA nucleic acid bases with fragments derived from CNTs (5, 5) and (10, 0). The CNT fragments were frozen with saturated H atoms, thus limiting the interaction of the CNT with the nucleic acid base. This will surely affect the binding energy of the nucleic acid base, whereas we have taken the fully relaxed CNT and allowed all the atoms to move freely in all three directions. Wang [18] reported more than one stable configuration of nucleic acid base on CNT, with a binding energy for guanine varying from 0.32 to 0.44 eV for CNT (5, 5) and from 0.22 to 0.34 eV for CNT (10, 0) without basis set superposition error (BSSE) correction. In another study using MP2 level theory, binding energies of guanine with CNT (5, 5) in the order of 0.36 to 0.88 eV were reported [13]. The curvature-free surface of graphene facilitates the adsorption of planar molecules compared to narrow nanotubes [29]. Except in the case of CNT (5, 0), the binding energy of guanine increases with increasing CNT diameter (Table 1).

Optimized structures of CNT+thymine complexes are presented in Fig. 2. The parallel orientation of thymine helps the interaction between the π orbitals of CNT and thymine. In the adsorption of thymine on CNT (5, 0), the upper half of thymine gets very close to the CNT (Fig. 2e). The lone pair of electrons present in the nitrogen and oxygen atoms caused a tilt in the parallel orientation of thymine on the CNT surface but still the thymine remains planar without pyramidalization. Due to π electron cloud interactions between the CNT and thymine, the CNT becomes distorted in the direction of the adsorbate, like in the CNT (5, 0)+G complex. Here the radius of the (5, 0) tube shrinks to 1.92 Å. In the other three cases , the adsorbate does not lead to any change in the CNT structure. Wang [18] analyzed the ability of thymine to disperse SWCNTs by investigating the adsorption of nucleic acid bases on CNT in the gas and aqueous phases. The reported binding energies in the gas phase using MPWBIK functional are in the range of 0.11 to 0.29 eV for the different orientations of thymine on CNT (5, 5), and these values agree well with our results (Table 1).

CNT (10, 0) is a wide tube, with a lesser curvature effect compared to the other nanotubes considered in this study. The binding energy of thymine with CNT (10, 0) is 0.20 eV. In a study of the interaction of thymine/thymine radicals with CNT (10, 0) [17], binding energies in the order of 0.22 to 0.31 eV are reported, which is comparable with our results. However, the binding energy of thymine with CNT (10, 0) is expected to be higher than the other narrow nanotubes. In the optimized structure of CNT (10, 0)+T (Fig. 2d), thymine is positioned at a distance of 2.46 Å. This is the shortest intermolecular distance of all the nanotubes tested here. Two CO and NH groups of thymine are tilted towards the CNT. The intermolecular distance between the adsorbent and adsorbate plays a key role in the π-stacking interaction. The π–π repulsive interaction between the adsorbent and adsorbate causes the system to have a certain distance of separation called the characteristic distance of π-stacking, so as to minimize the exchange repulsive interaction between them. Electronegative oxygen and nitrogen atoms present in thymine are thus dragged towards the CNT; this increases the repulsive interaction between the thymine and the CNT and results a considerable reduction in the binding energy.

Generally, π–π interaction energy is the result of electrostatic, induction, charge transfer, dispersion and repulsive energies between the adsorbent and adsorbate [30]. DFT fails to describe the dispersion interaction of

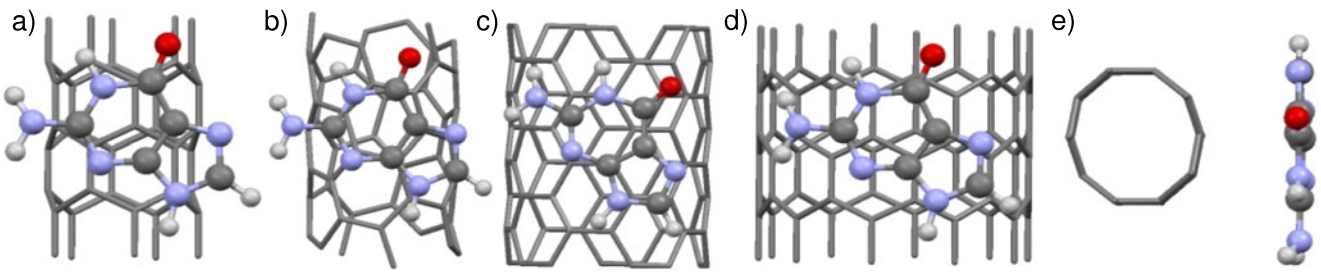

Fig. 1a–e Optimized configurations of guanine adsorbed on carbon nanotubes (CNTs). **a** CNT (5, 0)+G; **b** CNT (5, 2)+G; **c** CNT (5, 5)+G; **d** CNT (10, 0)+G; **e** CNT (5, 0)+G

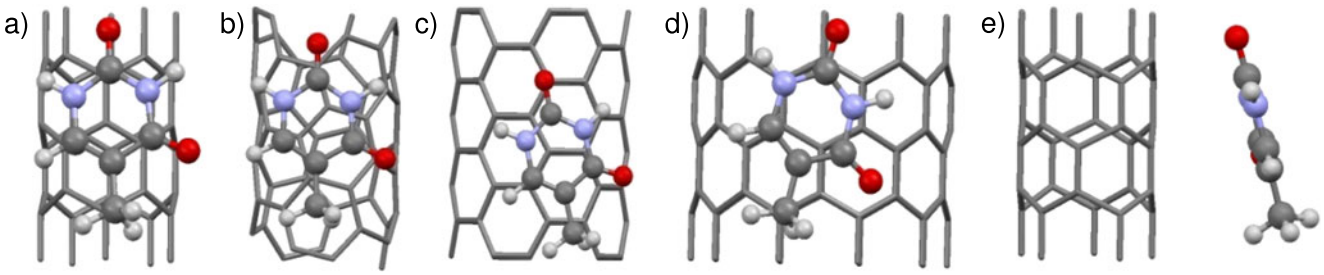

Fig. 2a–e Optimized configurations of thymine adsorbed on CNTs. **a** CNT (5, 0)+T; **b** CNT (5, 2)+T; **c** CNT (5, 5)+T; **d** CNT (10, 0)+T; **e** CNT (5, 0)+T

noncovalent systems at very large distances. Calculating the interaction energy perturbatively using symmetry-adapted perturbation theory (SAPT) [31] can describe such intermolecular interactions, including dispersion energy. SAPT interaction energy is expressed as the sum of electrostatic, exchange, induction, exchange-induction, dispersion and exchange-dispersion components. It is a very successful technique for molecules of ten atoms or fewer but is not suitable for large systems. In our case, the intermolecular separation between CNT and nucleic acid base varies between 2.46 and 3.26 Å. With this intermolecular separation, DFT-LDA can determine the interaction energy of the noncovalent system successfully [24]. Here, the binding energy results from electrostatic, induction, charge transfer and repulsive interactions.

Charge transfer and charge density analysis

Bader charge density analysis [32] was performed to determine the total charge associated with each atom and to investigate possible charge transformation between the two entities. Although there is no direct chemical bonding between the adsorbate and CNT, we can expect a fractional charge transfer between them due to the π electrons and lone pair of electrons. In a similar situation, Stepanian et al. [13] observed a downshift of G-band frequency in the Raman spectra due to partial charge transfer to the nanotube from the nucleic acid base. In our case, a charge of 0.09e is transferred to CNT (5, 0) from guanine (Table 1); this validates the higher binding energy of guanine with the narrow tube rather than the wide tubes. The high curvature surface and the increased electronegativity of CNT (5, 0) drag more electrons towards it [10]. In the other cases, there is no significant charge transfer.

In some earlier works, charge transfer between the CNT and the nucleic acid base was calculated [11, 14, 17, 18] and isosurface plots [11, 17] were examined. Physisorption of nucleic acid bases with CNT occurs due to the interaction between the π electron clouds. Thus, by concentrating on the complete charge density profile of CNT and nucleic acid bases, we will be able to give a better interpretation about the nature of the interaction between them. We analyzed [33] the highest occupied molecular orbital (HOMO) and lowest unoccupied molecular orbital (LUMO) surfaces of CNT and nucleic acid bases. Here, we present the results of two important as well as unique cases: adsorption of guanine on CNT (5, 0) and adsorption of thymine on CNT (10, 0). Figure 3 shows the charge density distribution of the isolated guanine molecule and CNT (5, 0) guanine hybrid.

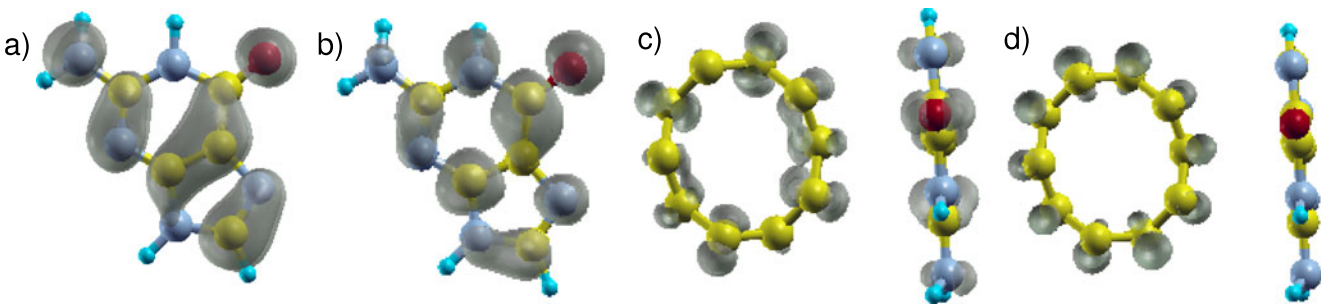

Fig. 3a–d Charge distribution in the CNT (5, 0) guanine hybrid. **a** Highest occupied molecular orbital (HOMO) of isolated guanine. **b** Lowest unoccupied molecular orbital (LUMO) of isolated guanine. **c** HOMO of CNT (5, 0) guanine hybrid. **d** LUMO of CNT (5, 0) guanine hybrid

Charge density is concentrated on the C–C and C–N bonds of the isolated HOMO guanine (Fig. 3a), and in LUMO (Fig. 3b) it spreads over all the atoms. Contribution of the delocalized π electrons of the CNT in the interaction is clearly visible in the bottom panel pictures. Contraction of the CNT diameter near the adsorption field disturbs the π electron distribution over the carbon atoms (Fig. 3c). Thus there is depletion in the charge density of HOMO, whereas in LUMO charge is distributed homogeneously throughout the CNT (Fig. 3d). HOMO charge density concentrated on the guanine triggers physisorption with CNT. Charge accumulated on the oxygen and C–N bonds of guanine induces charge transfer to CNT. HOMO and LUMO of isolated thymine and the CNT (10, 0) thymine hybrid are presented in Fig. 4. In the HOMO of the isolated molecule (Fig. 4a), the charge density is evenly distributed over the carbon, nitrogen and oxygen atoms. Accurate geometry optimization plays a crucial role in the study of non-covalent interactions. During the adsorption of thymine on CNT (10, 0), thymine tilts towards the CNT along the side with two oxygen atoms. In the HOMO (Fig. 4c) of CNT (10, 0)+Thymine, a large collection of π electron density is gathered on the CNT near the thymine. Also, some small amount of charge accumulates on the base. Thus, the interaction between the π electron clouds is repulsive, and reduces the binding strength between the two entities.

Electronic band structure and density of state analysis

Generally, the electronic property of a CNT is not modified by physisorption of the adsorbate [11, 17]. Figure 5 shows the electronic band structure and density of states plots for the CNT (5, 0) and CNT (5, 0) guanine hybrid and CNT (5, 0) thymine hybrid, respectively. Intrinsic CNT exhibits metallic characteristics; the adsorption of neither guanine nor thymine changes the electronic properties of CNT (5, 0). However, the adsorption of the nucleic acid bases introduced additional bands below −0.5 eV in the intrinsic CNT band structure. In the DOS plot, no changes were observed at the Fermi level, confirming that the adsorption of nucleic acid bases on CNT is a simple superposition of individual systems without hybridization of orbitals. This holds true for all the other cases too.

Interaction of guanine thymine pair with CNT (5, 0)

In addition to the study of the adsorption of isolated bases on CNT, adsorption of a single guanine-thymine (GT) wobble base pair on CNT (5, 0) was investigated. A GT wobble base pair is formed with two hydrogen bonds between the O–H–N atoms of the bases [8]. Zheng et al. [6, 7] proposed CNT sorting mediated through a poly GT oligonucleotide formed by a non-Watson-Crick hydrogen bond network. A study of adsorption of a GT dimer on

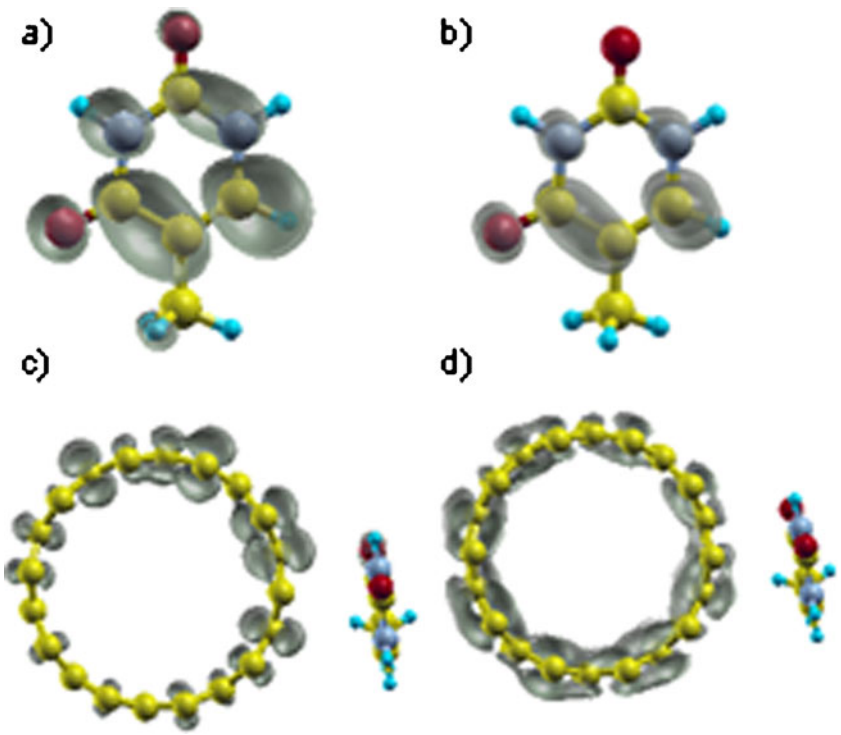

Fig. 4a–d Influence of the intermolecular separation in the charge accumulation and depletion in CNT (10,0) thymine hybrid. **a** HOMO of isolated thymine. **b** LUMO of isolated thymine. **c** HOMO of CNT (10, 0) thymine hybrid. **d** LUMO of CNT (10, 0) thymine hybrid

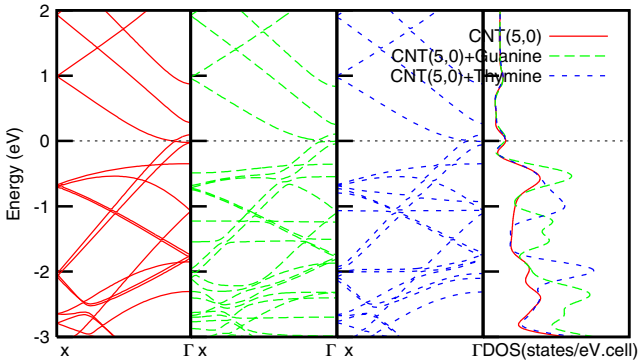

Fig. 5 Comparison between the band structure and density of states of CNT (5, 0), CNT (5, 0) guanine hybrid and CNT (5, 0) thymine hybrid

(11, 0) SWCNT revealed that, due to the stress induced within the ssDNA sugar residues and glycosidic bonds during optimization, the structural geometry was altered and became unstable [8]. In our study, the sugar phosphate backbone of DNA is not taken into account. Initially, the GT base pair is placed parallel to the CNT in the *z*-axis direction. The optimization process rearranged the initial parallel orientation of the base pair. The oxygen- and nitrogen-enriched middle portion of the nucleic acid base pair is moved away from the CNT (Fig. 6). Binding energy of the π–π stacked system is expected to increase in proportional with the π electron surface [30]. The calculated binding energy of the GT base pair with CNT (5, 0) is 0.36 eV. In comparison with the binding energy of isolated guanine (0.41 eV) and thymine (0.20 eV) with CNT (5, 0), the binding strength of the guanine thymine base pair on CNT (5, 0) is relatively weak. Charge density analysis has shown a charge transfer of 0.1e to the CNT from the base pair. The electronic charge density plots of HOMO and LUMO are presented in Fig. 6. In the HOMO (Fig. 6a), charge is distributed over the CNT and oxygen, nitrogen atoms of the nucleic acid bases. Charge of the LUMO (Fig. 6b) is distributed evenly on CNT, which establishes the metallic nature of the tube.

Conclusions

We have studied the interaction mechanism of the nucleic acid bases guanine and thymine with four different CNTs. Apart from the curvature effect of CNT, orientation of the nucleic acid bases and intermolecular distance between CNT and nucleic acid base play a predominant role in deciding the binding strength, which in turn influences charge transfer. Most importantly, the π–π stacking interaction is affected by the intermolecular distance between the CNT and the nucleic acid base. The binding strength of the nucleic acid base is reduced due to the exchange-repulsive interaction of the π–π charge cloud when the intermolecular distance between the adsorbent and adsorbate is less than the characteristic π–π stacking separation. However, the resultant π–π stacking interaction is attractive. When comparing the results obtained for guanine and thymine, the interaction energy of guanine is higher than that of thymine for all the CNTs tested. The role of van der Waals interactions in determining the magnitude of the π–π interaction energy is directly proportional to the area of the π overlap [30]. In addition to the pyrimidine ring of thymine, guanine has a fused imidazole ring and more electronegative nitrogen atoms, increasing the area of π surface of the adsorbate, which enhances the interaction. The binding energy of the adsorbate increases as the diameter of the CNT increases. However, this is not true in the case of guanine adsorption on CNT (5, 0) and thymine adsorption on CNT (10, 0). The high curvature of the narrow CNT (5, 0) drags more electrons towards it, and the contraction of the CNT facilitates the interaction of π electron clouds. This explains the higher binding energy of guanine with the narrow tube rather than the wide tubes. In

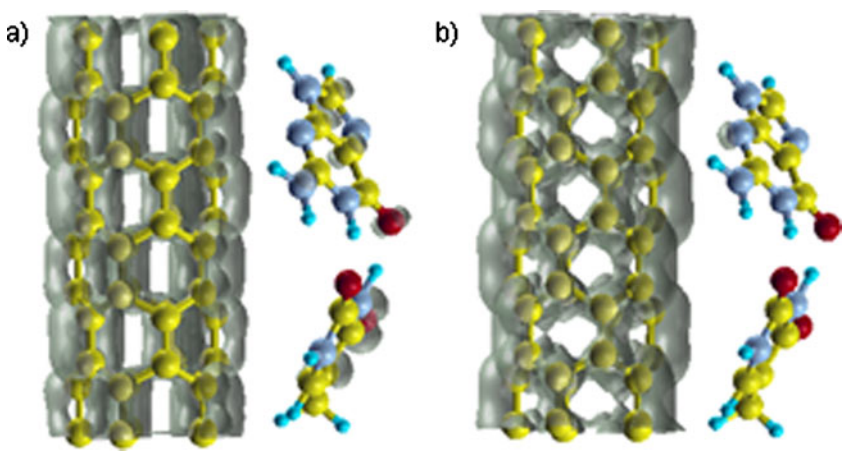

Fig. 6a,b Intermolecular interaction of CNT (5, 0) guanine thymine hybrid. **a** HOMO of CNT (5, 0) guanine thymine hybrid. **b** LUMO of CNT (5, 0) guanine thymine hybrid

the case of CNT (10, 0), the short intermolecular separation between thymine and CNT (10, 0) leads to the reduced binding energy of thymine because of the increased π–π repulsive interaction. Our results confirm that DFT-LDA can forecast the intermolecular separations and binding energies of non-covalent systems. Modeling a bio-nano hybrid like a non-covalently adsorbed nucleic acid base on CNT can lead to the utilization of CNT as a sensor or as a transporter for drugs and genes.

Acknowledgments The University Grants Commission is acknowledged for supporting this project with a junior research fellowship, under University with Potential for Excellence. K.I. acknowledges the financial support of the Council of Scientific and Industrial Research under the Emeritus Scientist Scheme. The authors would like to express their sincere thanks to the crew of the Center for Computational Materials Science at the Institute for Materials Research, Tohoku University, for their continuous support of the SR11000 supercomputing facilities.

References

1. Lu Q, Moore JM, Huang G, Mount AS, Rao AM (2004) RNA polymer translocation with single-walled carbon nanotubes. Nano Lett 4:2473–2477
2. Kam NWS, Dai H (2005) Carbon nanotubes as intracellular protein transporters: generality and biological functionality. J Am Chem Soc 127:6021–6026
3. Chen RJ, Bangsarunzip S, Drouvalakis KA, Shi Kam NW, Shim M, Li Y, Kim W, Utz PJ, Dai H (2003) Noncovalent functionalization of carbon nanotubes for highly specific electronic biosensors. Proc Natl Acac Sci USA 100:4984–4989
4. Kuang Z, Kim SN, Crookes-Goodson WJ, Farmer BL, Naik RR (2010) Biomimetic chemosensor: designing peptide recognition elements for surface functionalization of carbon nanotube field effect transistors. ACS Nano 4:452–458
5. Zheng M, Jagota A, Semke ED, Diner BA, Mclean RS, Lustig SR, Richardson RE, Tassi NG (2003) DNA-assisted dispersion and separation of carbon nanotubes. Nat Mater 2:338–342
6. Zheng M, Jagota A, Strano MS, Santos AP, Barone P, Chou SG, Diner BA, Dresselhaus MS, Mclean RS, Onoa GB, Samsonidze GG, Semke ED, Usrey M, Walls DJ (2003) Structure based carbon nanotube sorting by sequence-dependent DNA assembly. Science 302:1545–1548
7. Tu X, Zheng M (2008) A DNA based approach to the carbon nanotube sorting problem. Nano Res 1:185–194
8. Johnson RR, Charlie Johnson AT, Klein ML (2008) Probing the structure of DNA-carbon nanotube hybrids with molecular dynamics. Nano Lett 8:69–75
9. Lu G, Maragakis P, Kaxiras E (2005) Carbon nanotube interaction with DNA. Nano Lett 5:897–900
10. Meng S, Maragakis P, Papaloukas C, Kaxiras E (2007) DNA nucleoside interaction and identification with carbon nanotubes. Nano Lett 7:45–50
11. Gowtham S, Scheicher RH, Pandey R, Karna SP, Ahuja R (2008) First-principles study of physisorption of nucleic acid bases on small diameter carbon nanotubes. Nanotechnology 19 (6):125701
12. Shukla MK, Dubey M, Zakar E, Namburu R, Czyznikowska Z, Leszczynski J (2009) Interaction of nucleic acid bases with single-walled carbon nanotube. Chem Phys Lett 480:269–272
13. Stepanian SG, Karachevtsev MV, Glamazda AY, Karachevtsev VA, Adamowicz L (2009) Raman spectroscopy study and first-principles calculations of the interaction between nucleic acid bases and carbon nanotubes. J Phys Chem A 113:3621–3629
14. Das A, Sood AK, Maiti PK, Das M, Varadarajan R, Rao CNT (2008) Binding of nucleobases with single-walled carbon nanotubes: theory and experiment. Chem Phys Lett 453:266–273
15. Frischknecht AL, Martin MG (2008) Simulation of the adsorption of nucleotide monophosphates on carbon nanotubes in aqueous solution. J Phys Chem C 112:6271–6278
16. Martin W, Zhu W, Krilov G (2008) Simulation study of noncovalent hybridization of carbon nanotubes by single-stranded DNA in water. J Phys Chem B 112:16076–16089
17. Shtogun YV, Woods LM, Dovbeshko GI (2007) Adsorption of adenine and thymine and their radicals on single-wall carbon nanotubes. J Phys Chem C 111:18174–18181
18. Wang Y (2008) Theoretical evidence for the stringer ability of thymine to disperse SWCNT than cytosine adenine: self stacking bases vs their cross stacking with SWCNT. J Phys Chem C 112:14297–14305
19. Kresse G, Furthmuller J (1996) Efficient iterative schemes for ab initio total-energy calculations using a plane-wave basis set. Phys Rev B 54:11169–11186
20. Kresse G, Furthmuller J (1996) Efficiency of ab initio total energy calculations for metals and semiconductors using a plane-wave basis set. Comput Mater Sci 6:15–50
21. Blochl PE, Kresse G, Joubert J (1999) Projected augmented-wave method. From ultrasoft pseudopotentials to the projector augmented-wave method. Phys Rev B 50:17953–17979
22. Perdew JP, Zunger A (1981) Self-interaction correction to density-functional approximations for many-electron systems. Phys Rev B 23:5048–5079
23. Perdew JP, Chevary JA, Vosko SH, Jackson KA, Pederson MR, Singh DJ, Fiolhais C (1992) Atoms, molecules, solids, and surfaces: applications of the generalized gradient approximation for exchange and correlation. Phys Rev B 46:6671–6687
24. Girifalco LA, Hodak M (2002) Van der Waals binding energies in graphitic structures. Phys Rev B 65(1):125404
25. Tournus F, Latil S, Heggie MI, Charlier JC (2005) π-stacking interaction between carbon nanotubes and organic molecules. Phys Rev B 72(5):075431
26. Ortmann F, Schmidt WG, Bechstedt F (2005) Attracted by long range electron correlation: adenine and graphite. Phys Rev Lett 95 (4):186101
27. Lim S, Park N (2009) Ab initio study of noncovalent sidewall functionalization of carbon nanotubes. Appl Phys Lett 95(3):243110
28. Monkhorst HJ, Pack JD (1976) Special points for brillouin-zone integrations. Phys Rev B 13:5188–5192
29. Liu Z, Sun X, Nakayama-Ratchford N, Dai H (2007) Supramolecular chemistry on water-soluble carbon nanotubes for drug loading and delivery. ACS Nano 1:50–56
30. Hunter CA, Sanders JKM (1990) The nature of π–π interactions. J Am Chem Soc 112:5525–5534
31. Jeziorski B, Moszynski R, Szalewicz K (1994) Perturbation theory approach to intermolecular potential energy surfaces of van der Waals complexes. Chem Rev 94:1887–1930
32. Henkelman G, Arnaldsson A, Jonsson H (2006) A fast and robust algorithm for Bader decomposition of charge density. Comput Mater Sci 36:254–360
33. Kokalj A (2003) Computer graphics and graphical user interfaces as tools in simulations of matter at the atomic scale. Comput Mater Sci 28:155–168